

Evaluating aspects of the Community Land and Atmosphere Models (CLM3 and CAM3)

using a dynamic global vegetation model

Gordon B. Bonan and Samuel Levis

National Center for Atmospheric Research

Boulder Colorado

USA

Corresponding Author:

Gordon Bonan
National Center for Atmospheric Research
PO Box 3000
Boulder CO 80307-3000
USA
Tel. 303 497-1613
Fax. 303 497-1695
Email: bonan@ucar.edu

For JCLI CCSM special issue

Submitted December 2004

Revised June 2005

Abstract

The Community Land Model (CLM3) Dynamic Global Vegetation Model (CLM-DGVM) is used diagnostically to identify land and atmospheric model biases that lead to biases in the simulated vegetation. The CLM-DGVM driven with observed atmospheric data (offline simulation) underestimates global forest cover, overestimates grasslands, and underestimates global net primary production. These results are consistent with earlier findings that the soils in CLM3 are too dry. In the offline simulation an increase in simulated transpiration by changing this variable's soil moisture dependence and by decreasing canopy-intercepted precipitation results in better global plant biogeography and global net primary production. When CLM-DGVM is coupled to the Community Atmosphere Model (CAM3), the same modifications do not improve simulated vegetation in eastern United States and Amazonia where the most serious vegetation biases appear. The dry bias in eastern United States precipitation is so severe that the simulated vegetation is insensitive to changes in the hydrologic cycle. In Amazonia, strong coupling among soil moisture, vegetation, evapotranspiration, and precipitation produces a highly complex hydrologic cycle in which small perturbations in precipitation are accentuated by vegetation. These interactions in Amazonia lead to a dramatic precipitation decrease and a collapse of the forest. These results suggest that the accurate parameterization of convection poses a complex and challenging scientific issue for climate models that include dynamic vegetation. The results also emphasize the difficulties that may arise when coupling any two highly non-linear systems that have only been tested uncoupled.

1. Introduction

Dynamic global vegetation models (DGVMs) were introduced as a practical and ecologically realistic means of simulating vegetation change in global climate models (Foley et al. 1996; Friend et al. 1997; Brovkin et al. 1997; Cox et al. 1998; Potter and Klooster 1999; Kucharik et al. 2000; Sitch et al. 2003; Bonan et al. 2003). DGVMs coupled to climate models have been used to simulate vegetation for past, present, and future climates to assess the interactions among climate, CO₂, and vegetation (Levis et al. 1999, 2004b; Doherty et al. 2000; Brovkin et al. 2003; Wang et al. 2004; Cowling et al. 2004). DGVMs have also been used in offline simulations (not coupled to a climate model), usually to evaluate simulated vegetation against observations and other model simulations (e.g., Cramer et al. 2001).

The vegetation simulated by DGVMs responds primarily to solar radiation, air temperature, and soil moisture (in this paper, we neglect the response to changing atmospheric CO₂ concentration). Therefore, the successful coupling of a DGVM to a climate model to simulate climate-vegetation feedbacks relies on good quality atmospheric and soil moisture data in addition to the careful selection of vegetation parameterizations. In this paper, we use a DGVM to identify key land and atmosphere biases in the Community Climate System Model (CCSM3) that result in large biases in simulated vegetation.

2. Methods

a. Models

We use the Community Land Model version 3 (CLM3) (Oleson et al. 2004) with dynamic vegetation (Levis et al. 2004a). The model, hereafter referred to as CLM-DGVM, is coupled to the Community Atmosphere Model version 3 (CAM3) (Collins et al. 2005) with a 20-minute time step. CAM3 is a spectral model and here CAM3 and CLM-DGVM operate at T42 horizontal resolution ($\sim 2.81^\circ$ by 2.81° in longitude and latitude). Dickinson et al. (2005) describe biases in the land surface climatology. In this paper we are primarily interested in prominent dry biases in eastern United States and tropical South American precipitation. For our simulations, we use climatological sea surface temperatures and sea ice rather than the fully coupled CCSM3, but the specific dry and associated warm biases persist (Figure 1).

The DGVM is the same used with the NCAR LSM land surface model, which is the predecessor to the Community Land Model, and has been documented and evaluated against observations (Bonan et al. 2003). The dynamic vegetation parameterizations originated mostly from the LPJ-DGVM, a model also documented and evaluated against observations (Sitch et al. 2003). LSM-DGVM and LPJ-DGVM simulate similar global vegetation with a tendency in LSM-DGVM to overestimate global net primary production and forest cover at the expense of grasses. CLM-DGVM, when forced with the same prescribed atmospheric data as LSM-DGVM, underestimates global net primary production and forest cover and favors grasses (Levis et al. 2004a). We hypothesize that the difference in simulated vegetation between CLM-DGVM and LSM-DGVM relates to aspects of the simulated soil moisture.

CLM3, CLM-DGVM, and CAM3 are described at length elsewhere (Oleson et al. 2004; Levis et al. 2004a; Collins et al. 2005). Here we restrict our model description to two CLM3 parameterizations previously identified as causing the model to have drier soils than NCAR LSM (Bonan et al. 2002a). We describe modifications to these parameterizations such that more soil moisture may be transpired during plant photosynthesis and more precipitation may reach the soil. The first pertains to the soil water factor, β_t , and the second to the fraction of canopy-intercepted precipitation, f_{pi} :

1) β_t is a coefficient in the calculation of the maximum rate of carboxylation, V_{max} , a key variable in the photosynthesis calculation and by extension the transpiration calculation (Oleson et al. 2004). β_t ranges nonlinearly from 0 to 1 as a function of soil water based on matric potential and root resistance. Lower values of β_t decrease the rate of photosynthesis, stomatal conductance, and transpiration, all other factors being equal. For the purpose of this study we have modified β_t to a linear function of soil water from wilting point ($\beta_t = 0$) to optimum transpiration ($\beta_t = 1$), as in NCAR LSM (Bonan 1996). In CLM3 β_t for a given soil moisture is always less than or equal to that in NCAR LSM and the difference grows for drier soil (Bonan et al. 2002a).

2) Both CLM3 and NCAR LSM have the same maximum canopy water storage (0.1 mm per unit leaf and stem area), but NCAR LSM restricts interception to 20% of precipitation (Bonan et al. 2002a). In CLM3 the maximum fraction of precipitation intercepted by vegetation increases with leaf area index (L) and stem area index (S) as $f_{pi} = 1 - \exp[-0.5(L + S)]$. In CLM3 f_{pi} exceeds that of NCAR LSM for $(L + S)$ greater than about $0.45 \text{ m}^2 \text{ m}^{-2}$, which is the case in all but the most arid regions of the world. At leaf and stem area index greater than about $4.5 \text{ m}^2 \text{ m}^{-2}$, CLM3 allows more than 90% of

precipitation to be intercepted (if storage capacity is not exceeded). Greater canopy interception means that less precipitation reaches the ground. Greater interception also results in a greater wetted leaf fraction, which reduces the leaf surface area from which transpiration occurs. For the purpose of this study we have modified f_{pi} to that used in NCAR LSM.

b. Simulations

We performed three sets of paired climate model simulations to identify deficiencies in the CAM3 climate and the CLM3 hydrologic cycle that adversely affect the global plant biogeography simulated by CLM-DGVM. The first two sets of simulations utilized the dynamic vegetation, forced with either observed atmospheric data or coupled to CAM3:

- 1a. (OV) 80-year offline CLM-DGVM simulation forced with observed atmospheric data from the period 1979-1998 (Bonan et al. 2002b). The 20-year atmospheric data was cycled to allow an 80-year simulation.
- 1b. (OVM) 120-year offline CLM-DGVM simulation with β_1 and f_{pi} modified as per section 2a.
- 2a. (CV) 120-year simulation like OV but coupled to CAM3.
- 2b. (CVM) 120-year simulation like OVM but coupled to CAM3.

The third set of simulations disabled the dynamic vegetation as in the standard CAM3-CLM3:

- 3a. (C) 50-year simulation like CV but without vegetation dynamics. Vegetation is prescribed from satellite data as in CLM3 when run without dynamic vegetation

(Bonan et al. 2002a; Levis et al. 2004a). This is the standard CAM3-CLM3 configuration.

3b. (CM) 20-year simulation like C but with β_t and f_{pi} modified.

Simulation OVM relative to simulation OV reveals the combined role of β_t and f_{pi} on global vegetation. Simulations CV and CVM compared to OV and OVM isolate the role of climate biases relative to the role of β_t and f_{pi} on global vegetation. Simulations C and CM isolate the climatic effects of changes to β_t and f_{pi} independent of vegetation dynamics.

All simulations with dynamic vegetation enabled were initialized from a previous spin-up simulation. Starting from bare ground, CLM-DGVM vegetation was brought to equilibrium in a 400-year simulation at T31 horizontal resolution ($\sim 3.75^\circ$ by 3.75° in longitude and latitude) driven with the atmospheric data used also in OV and OVM. Output from this simulation was mapped to T42 horizontal resolution ($\sim 2.81^\circ$ by 2.81°) to initialize OV. Land surface initial conditions for the remaining simulations were obtained from OV.

3. Results and Discussion

a. Vegetation simulated with prescribed atmospheric data

Results from simulation OV illustrate that CLM-DGVM underestimates forest cover on a global scale in favor of grasses (Figures 2, 3a). In areas where forests are simulated, especially in the tropics, CLM-DGVM underestimates evergreen trees in favor of deciduous trees. Observed vegetation includes crops and shrubs. Simulated vegetation does not, which explains many of the large differences from the observations. However,

the dominance of deciduous trees where one would expect evergreens in the tropics, the dominance of grasses instead of trees in eastern United States, and the dominance of grasses in mid-continental parts of the boreal forest all suggest the soils are simulated too dry to support observed vegetation. The global total net primary production (43 Pg C yr^{-1}) is 25-30% lower than observational estimates (Schlesinger 1997). These results are in contrast to simulations with LSM-DGVM, which showed more geographically extensive and more productive forest vegetation (Bonan et al. 2003).

Simulation OVM uses two parameterizations from LSM-DGVM that allow more precipitation to reach the soil and more soil water to be accessed by plants for photosynthesis and transpiration (section 2a). As a result coefficient β_i increases, canopy evaporation decreases, and transpiration increases compared with OV (Figure 4). Transpiration increases because the higher values of β_i allow higher stomatal conductance, but also because less precipitation is intercepted by foliage so that the wetted fraction of the canopy, from which transpiration is precluded, decreases. Simulation OVM produces increased forest cover and reduced grass cover compared with OV in agreement with our hypothesis that the soils in CLM-DGVM are too dry (Figure 3). The relative distribution of evergreen and deciduous trees has not reached equilibrium, but the trends on a global average (not shown) decrease for most plant functional types over the course of the simulation, indicating that global biogeography is approaching steady state. Evergreen trees occupy more of the tropical rainforest, trees dominate the eastern United States, and trees appear in mid-continental areas of the boreal forest (Figure 3b versus Figure 3a). The global total net primary production (60 Pg C yr^{-1}) is in good agreement with published estimates of this variable (Schlesinger 1997).

b. Vegetation simulated with CAM3

Simulations CV and CVM couple CLM-DGVM to CAM3. The global vegetation patterns simulated in CV and OV are similar in that forest cover is underestimated and grass cover is overestimated (Figure 5a versus Figure 3a). Regionally there are differences that are directly related to biases in simulated precipitation (Figure 6). For example, the Amazon rainforest is even more deciduous in CV than in OV due to a dry bias in precipitation. The eastern United States is drier in CV compared with OV resulting in even fewer trees. Some desert appears in central United States. Elsewhere, a wet bias contributes to denser vegetation than in OV. This is particularly evident in tropical Africa, Indonesia, and China, where forests are denser, and in southern Africa, the Arabian Peninsula, and northern Australia, where grasses are denser. The global total net primary production (53 Pg C yr^{-1}) is higher than in OV due to overestimated precipitation in CV in most regions other than eastern United States and Amazonia (Figure 6).

Simulation CVM shows the same general characteristics of OVM, with reduced canopy evaporation and increased transpiration compared with CV, but the soil water factor β_t does not increase greatly and it decreases in some regions such as Amazonia (Figure 7). Simulation CVM preserves some of the characteristics of global vegetation found in CV, but the dry and warm biases in eastern United States and the Amazon basin are more extreme (Figure 6c and 6f). As a result vegetation patterns simulated in CV persist or degrade in CVM (Figure 5). Only forest cover at higher latitudes increases in

response to the modified CLM3 parameterizations. Global total net primary production is 61 Pg C yr^{-1} .

c. On climate-vegetation coupling in CLM-DGVM and CAM3

Why does the model's dry bias in Amazonia intensify in response to the modified CLM3 parameterizations in CVM? Offline model simulations OV and OVM show that less water evaporates from the canopy and more transpires through leaf stomata with the modifications to β_l and f_{pi} (Figure 4). In part, this is because the wetted fraction of the canopy is reduced, but transpiration also increases because β_l increases. However, total evapotranspiration (the sum of transpiration and soil and canopy evaporation) decreases and runoff increases, in part because less water is intercepted and more water reaches the soil (Table 1). Coupled model simulations C and CM, with prescribed rather than dynamic vegetation, show similar behavior with reduction in total evapotranspiration in Amazonia (Figure 8, Table 1).

In CV and CVM the reduction in total evapotranspiration in combination with the dynamic vegetation initiates a positive feedback that reduces precipitation in Amazonia (Table 1). This decrease in the intensity of the hydrologic cycle coincides with a decline in forest vegetation and an increase in grasses. Simulation CV maintains a landscape that is primarily forest (55% tree, 37% grass). Simulation CVM has 25% tree cover and 60% grass cover (Table 1). The decline in tree cover and increase in grass cover is abrupt, occurring within the first two years of the simulation. The reduction in evapotranspiration with the modifications to CLM3 reduces precipitation, which further dries the soil and causes a dieback of forest vegetation, which further reduces evapotranspiration. Other

studies have also shown that CAM3 and CLM3 have high land-atmosphere coupling strength in this region such that precipitation is sensitive to perturbations in soil moisture and evapotranspiration (Koster et al. 2005; Guo et al. 2005). Such a decrease in precipitation is not seen in simulations C and CM, which used prescribed vegetation datasets, suggesting that the conversion of forest to grassland with the drier climate contributed to the reduction in precipitation (Table 1).

Similar behavior is seen in eastern United States. The modifications to CLM3 reduce evapotranspiration and increase runoff in the offline simulation OVM compared with OV, a trend that is accentuated in the coupled simulation CM (compared with C) due to decreased precipitation (Table 2). Here, however, the inclusion of dynamic vegetation in simulation CVM does not produce a large further decrease in precipitation (Table 2). The dry bias in eastern United States is so severe that the simulated vegetation of grassland (in contrast to observed forest) is insensitive to changes in the hydrologic cycle. Indeed, even a smaller reduction of 10% or 20% in annual precipitation begins to convert the forest vegetation to grassland (Table 3).

Except for these two regions (Amazonia, eastern United States), much of the rest of the world is subject to a wet precipitation bias in simulation CV without indications of strong feedbacks in simulation CVM except in North Africa (Figure 6). In this region climate is particularly sensitive to increased soil moisture and a positive feedback is established. More soil moisture lowers the surface albedo and intensifies the North African monsoon (Levis et al. 2004b).

4. Conclusions

Offline simulations in which CLM-DGVM is forced with observed atmospheric data indicate that this model's simulated vegetation is highly sensitive to land model parameterizations that affect the water cycle. In Amazonia, where CLM-DGVM underestimates evergreen tree cover, parameterization changes reducing canopy interception and increasing transpiration lead to an increase in evergreen tree cover. In southeast United States and in mid-continental boreal regions, where CLM-DGVM underestimates tree cover, the tree cover increases. These results along with satisfactory results from LSM-DGVM (Bonan et al. 2003) and LPJ-DGVM (Sitch et al. 2003) offer confidence in the ability of this model to simulate global vegetation when given observed climate.

Coupled simulations with CAM3 show that the simulated climate mostly overrides the effects of changing land model parameterizations. The vegetation of boreal regions, where CAM3 overestimates precipitation, shows improvement with the CLM3 parameterization changes as in the offline case. However, the vegetation of eastern United States and Amazonia does not. In these regions CAM3 has a dry and warm bias. The bias intensifies with the parameterization changes due to a hydrologic feedback that weakens the already weak hydrologic cycle of these regions. Dynamic vegetation further accentuates this feedback in Amazonia where dry soil reduces vegetation cover, which further reduces precipitation.

The results of these simulations suggest that the accurate parameterization of convection will pose an extremely complex scientific challenge for climate models that include vegetation feedbacks. In eastern United States, a 10% decrease in annual

precipitation from observations results in simulated vegetation that is parkland rather than forest, and a 20% reduction results in a savanna-like mixture of grasses and trees. Accurate simulation of vegetation in this region requires a high level of accuracy in the simulated precipitation. In Amazonia, strong coupling among soil moisture, vegetation, evapotranspiration, and precipitation produces a highly complex hydrologic cycle in which small perturbations in precipitation are accentuated by vegetation.

The results also emphasize the difficulties that may arise when coupling any two highly non-linear systems that have only been tested uncoupled. In particular, the two simple changes to the hydrologic cycle that performed well in the uncoupled CLM-DGVM performed poorly when coupled to CAM3. Future development of the hydrologic cycle in CLM3 will require an approach that improves vegetation and hydrology in both uncoupled and coupled simulations.

Acknowledgments

Computational facilities have been provided by the National Center for Atmospheric Research (NCAR). NCAR is supported by the National Science Foundation.

References

- Bonan, G. B., 1996: A land surface model (LSM version 1.0) for ecological, hydrological, and atmospheric studies: technical description and user's guide. NCAR Tech. Note NCAR/TN-417+STR, 150 pp.
- Bonan, G. B., K. W. Oleson, M. Vertenstein, and S. Levis, 2002a: The land surface climatology of the Community Land Model coupled to the NCAR Community Climate Model. *J. Climate*, **15**, 3123-3149.
- Bonan, G. B., S. Levis, L. Kergoat, and K. W. Oleson, 2002b: Landscapes as patches of plant functional types: an integrating concept for climate and ecosystem models. *Global Biogeochem. Cycles*, **16**, 1021, doi:10.1029/2000GB001360.
- Bonan, G. B., S. Levis, S. Sitch, M. Vertenstein, and K. W. Oleson, 2003: A dynamic global vegetation model for use with climate models: concepts and description of simulated vegetation dynamics. *Global Change Biol.*, **9**, 1543-1566.
- Brovkin, V., A. Ganopolski, and Y. Svirezhev, 1997: A continuous climate-vegetation classification for use in climate-biosphere studies. *Ecol. Model.*, **101**, 251-261.
- Brovkin, V., S. Levis, M.-F. Loutre, M. Crucifix, M. Claussen, A. Ganopolski, C. Kubatzki, and V. Petoukhov, 2003: Stability analysis of the climate-vegetation system in the northern high latitudes. *Climatic Change*, **57**, 119-138.
- Collins, W. D., P. J. Rasch, B. A. Boville, J. J. Hack, J. R. McCaa, D. L. Williamson, B. Briegleb, C. Bitz, S.-J. Lin, M. Zhang, and Y. Dai, 2005: The formulation and atmospheric simulation of the Community Atmosphere Model: CAM3. *J. Climate*, this issue.

- Cowling, S. A., R. A. Betts, P. M. Cox, V. J. Ettwein, C. D. Jones, M. A. Maslin, and S. A. Spall, 2004: Contrasting simulated past and future responses of the Amazonian forest to atmospheric change. *Philos. T. Roy. Soc. B*, **359**, 539-547.
- Cox, P. M., C. Huntingford, and R. J. Harding, 1998: A canopy conductance and photosynthesis model for use in a GCM land surface scheme. *J. Hydrol.*, **213**, 79-94.
- Cramer, W., A. Bondeau, F. I. Woodward, I. C. Prentice, R. A. Betts, V. Brovkin, P. M. Cox, V. Fisher, J. A. Foley, A. D. Friend, C. Kucharik, M. R. Lomas, N. Ramankutty, S. Sitch, B. Smith, A. White, and C. Molling-Young, 2001: Global response of terrestrial ecosystem structure and function to CO₂ and climate change: results from six dynamic global vegetation models. *Global Change Biol.*, **7**, 357-373.
- Dickinson, R.E., K.W. Oleson, G. Bonan, F. Hoffman, P. Thornton, M. Vertenstein, Z.-L. Yang, and X. Zeng, 2005: The Community Land Model and its climate statistics as a component of the Community Climate System Model. *J. Climate*, this issue.
- Doherty, R., J. E. Kutzbach, J. A. Foley, and D. Pollard, 2000: Fully coupled climate/dynamical vegetation model simulations over Northern Africa during the mid-Holocene. *Clim. Dynam.*, **16**, 561-573.
- Foley, J. A., I. C. Prentice, N. Ramankutty, S. Levis, D. Pollard, S. Sitch, and A. Haxeltine, 1996: An integrated biosphere model of land surface processes, terrestrial carbon balance, and vegetation dynamics. *Global Biogeochem. Cycles*, **10**, 603-628.

- Friend, A. D., A. K. Stevens, R. G. Knox, and Cannell, M. G. R., 1997: A process-based, terrestrial biosphere model of ecosystem dynamics (Hybrid v3.0). *Ecol. Model.*, **95**, 249-287.
- Guo, Z., P.A. Dirmeyer, R.D. Koster, G. Bonan, E. Chan, P. Cox, T. Gordon, S. Kanae, E. Kowalczyk, D. Lawrence, P. Liu, C.-H. Lu, S. Malyshev, B. McAvaney, J.L. McGregor, K. Mitchell, D. Mocko, T. Oki, K. Oleson, A. Pitman, Y.C. Sud, C.M. Taylor, D. Verseghy, R. Vasic, Y. Xue, and T. Yamada, 2005: GLACE: The Global Land-Atmosphere Coupling Experiment. 2: Model characteristics and comparison. *J. Hydrometeorology*, submitted.
- Koster, R.D., Z. Guo, P.A. Dirmeyer, G. Bonan, E. Chan, P. Cox, H. Davies, T. Gordon, S. Kanae, E. Kowalczyk, D. Lawrence, P. Liu, C.-H. Lu, S. Malyshev, B. McAvaney, K. Mitchell, D. Mocko, T. Oki, K. Oleson, A. Pitman, Y.C. Sud, C.M. Taylor, D. Verseghy, R. Vasic, Y. Xue, and T. Yamada, 2005: GLACE: The Global Land-Atmosphere Coupling Experiment. 1: Overview and results. *J. Hydrometeorology*, submitted.
- Kucharik, C. J., J. A. Foley, C. Delire, V. A. Fisher, M. T. Coe, J. D. Lenters, C. Young-Molling, N. Ramankutty, J. M. Norman, and S. T. Gower, 2000: Testing the performance of a Dynamic Global Ecosystem Model: Water balance, carbon balance, and vegetation structure. *Global Biogeochem. Cycles*, **14**, 795-825.
- Levis, S., G. B. Bonan, M. Vertenstein, and K. W. Oleson, 2004a: The Community Land Model's dynamic global vegetation model (CLM-DGVM): technical description and user's guide. NCAR Tech. Note TN-459+IA, 50 pp.

- Levis, S., J. A. Foley, and D. Pollard, 1999: CO₂, climate, and vegetation feedbacks at the Last Glacial Maximum. *J. Geophys. Res. -Atmos.*, **104**, 31191-31198.
- Levis, S., G. B. Bonan, and C. Bonfils, 2004b: Soil feedback drives the Mid-Holocene North African monsoon northward in fully coupled CCSM2 simulations with a dynamic vegetation model. *Clim. Dynam.*, doi:10.1007/s00382-004-0477-y.
- Oleson, K. W., Y. Dai, and Coauthors, 2004: Technical description of the Community Land Model (CLM). NCAR Tech. Note TN-461+STR, 174 pp.
- Potter, C. S., and S. A. Klooster, 1999: Dynamic global vegetation modelling for prediction of plant functional types and biogenic trace gas fluxes. *Global Ecol. Biogeogr.*, **8**, 473-488.
- Schlesinger, W. H., 1997: *Biogeochemistry : An Analysis of Global Change*. 2d ed. Academic Press, 588 pp.
- Sitch, S., B. Smith, I. C. Prentice, A. Arneth, A. Bondeau, W. Cramer, J. O. Kaplan, S. Levis, W. Lucht, M. T. Sykes, K. Thonicke, S. Venevsky, 2003: Evaluation of ecosystem dynamics, plant geography and terrestrial carbon cycling in the LPJ dynamic global vegetation model. *Global Change Biol.*, **9**, 161-185.
- Wang, G., E. A. B. Eltahir, J. A. Foley, D. Pollard, and S. Levis, 2004: Decadal variability of rainfall in the Sahel: results from the coupled GENESIS-IBIS atmosphere-biosphere model. *Clim. Dynam.*, **22**, 625-637.
- Willmott, C.J., and K. Matsuura, 2000: Terrestrial air temperature and precipitation: monthly and annual climatologies. [Available online at <http://climate.geog.udel.edu/~climate/>.]

Figures

Figure 1. Simulated and observed monthly temperature and precipitation for eastern United States (30-45°N, 70-100°W) and the Amazon basin (9°S-9°N, 52-75°W). Observations are from Willmott and Matsuura (2000).

Figure 2. Observed global vegetation cover as a percentage of the soil-covered portion of the grid cell (Bonan et al. 2002b).

Figure 3. As in Figure 2 but for vegetation in simulations (A) OV and (B) OVM. Data are averages from the last 20 years of each simulation.

Figure 4. Annual average (A) soil water factor, β , (B) evaporation of canopy-intercepted water (mm d^{-1}), and (C) transpiration (mm d^{-1}) from simulations OV and OVM. Data are averages from the last 20 years of each simulation.

Figure 5. As in Figure 3 but for simulations (A) CV and (B) CVM.

Figure 6. Annual average (A) observed precipitation from the data that drives simulations OV and OVM (Bonan et al. 2002b); (B) precipitation simulated in CV minus observed as a percent of the observed; (C) precipitation simulated in CVM minus that simulated in CV as a percent of that simulated in CV; (D) surface air temperature simulated in OV; (E) surface air temperature simulated in CV minus that simulated in OV; (F) surface air temperature simulated in CVM minus that simulated in CV. Data are averages from the last 20 years of each simulation.

Figure 7. As in Figure 4 but for simulations CV and CVM.

Figure 8. As in Figure 4 but for simulations C and CM.

Table 1. Annual average precipitation (P), evapotranspiration (E), and runoff (R) in simulations OV, OVM, CV, CVM, C, and CM for the Amazon basin (9°S-9°N, 52-75°W). Data are 20-year averages. The precipitation of OV and OVM is the observed precipitation (Bonan et al. 2002b). Observed runoff is from Dickinson et al. (2005). Also shown is the percent cover of evergreen trees (ET), deciduous trees (DT), and grasses (G) for simulations with dynamic vegetation. Observed vegetation is shown in Figure 2.

Simulation	P (mm d ⁻¹)		E (mm d ⁻¹)	R (mm d ⁻¹)		Vegetation cover (%) ET/DT/G
	Simulated	Observed		Simulated	Observed	
OV	-	5.88	3.81	2.07	3.81	27/56/15
OVM	-	5.88	2.64	3.24		42/49/8
CV	5.21		3.43	1.78		11/44/37
CVM	4.42		2.88	1.54		2/23/60
C	5.08		3.44	1.65		-
CM	5.16		3.11	2.06		-

Table 2. As in Table 1 but for eastern United States (30-45°N, 70-100°W).

Simulation	P (mm d ⁻¹)		E (mm d ⁻¹)	R (mm d ⁻¹)		Vegetation cover (%) ET/DT/G
	Simulated	Observed		Simulated	Observed	
	OV	-	2.75	1.83	0.93	
OVM	-	2.75	1.64	1.11		10/49/39
CV	1.99		1.66	0.33		0/0/65
CVM	1.82		1.52	0.29		0/2/78
C	2.08		1.81	0.27		-
CM	1.83		1.57	0.27		-

Table 3. Percent vegetation cover for eastern United States (30-45°N, 70-100°W) simulated with the modified CLM-DGVM under conditions of reduced precipitation. Data are for offline simulations (OVM) with annual precipitation reduced to 90%, 80%, 70%, and 60% of observed values. Data are averages from the last 20 years of each simulation.

Precipitation (% of observed)	Percent Vegetation Cover			
	Evergreen Tree	Summertime Tree	Grass	Bare
100 (OVM)	10	49	39	2
90	9	42	47	2
80	4	27	67	2
70	1	15	81	3
60	0	4	88	8

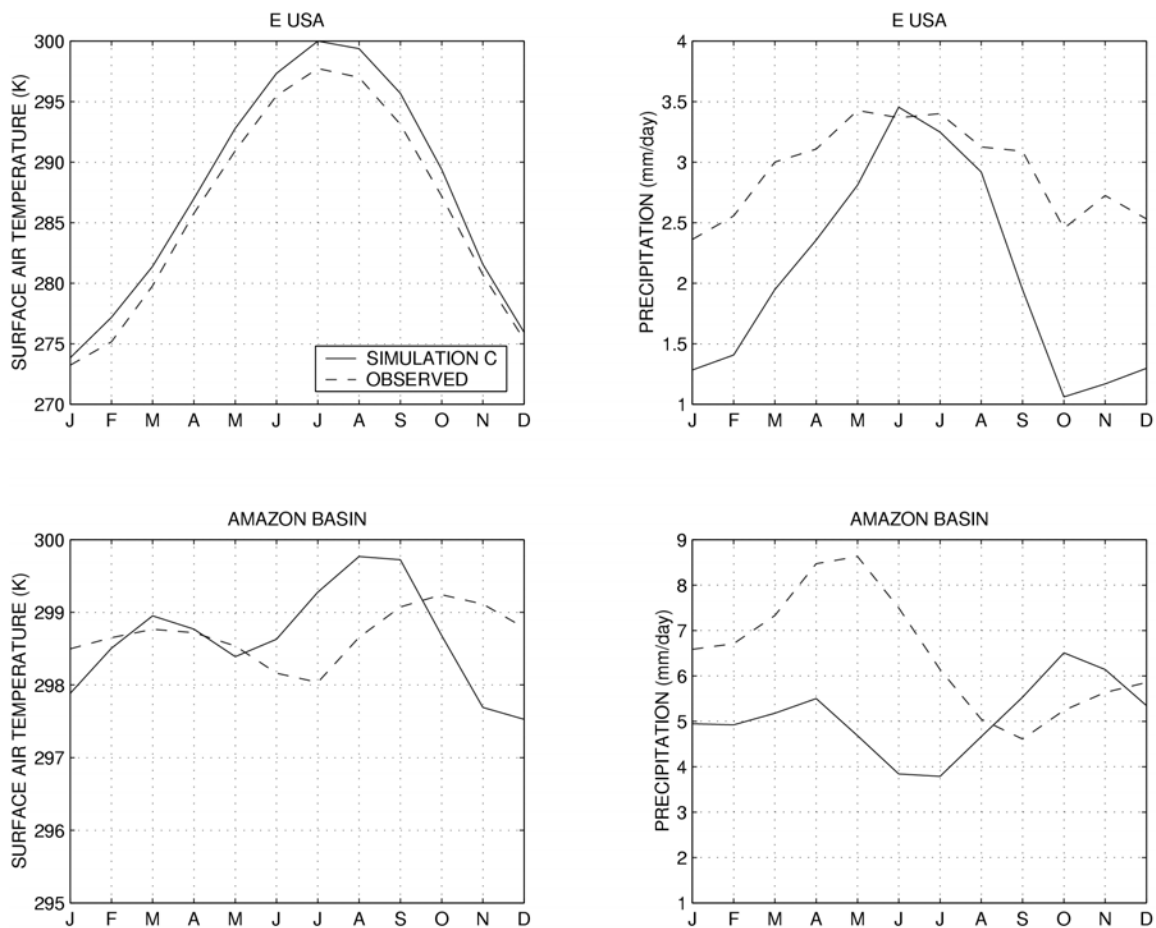


Figure 1. Simulated and observed monthly temperature and precipitation for eastern United States (30-45°N, 70-100°W) and the Amazon basin (9°S-9°N, 52-75°W). Observations are from Willmott and Matsuura (2000).

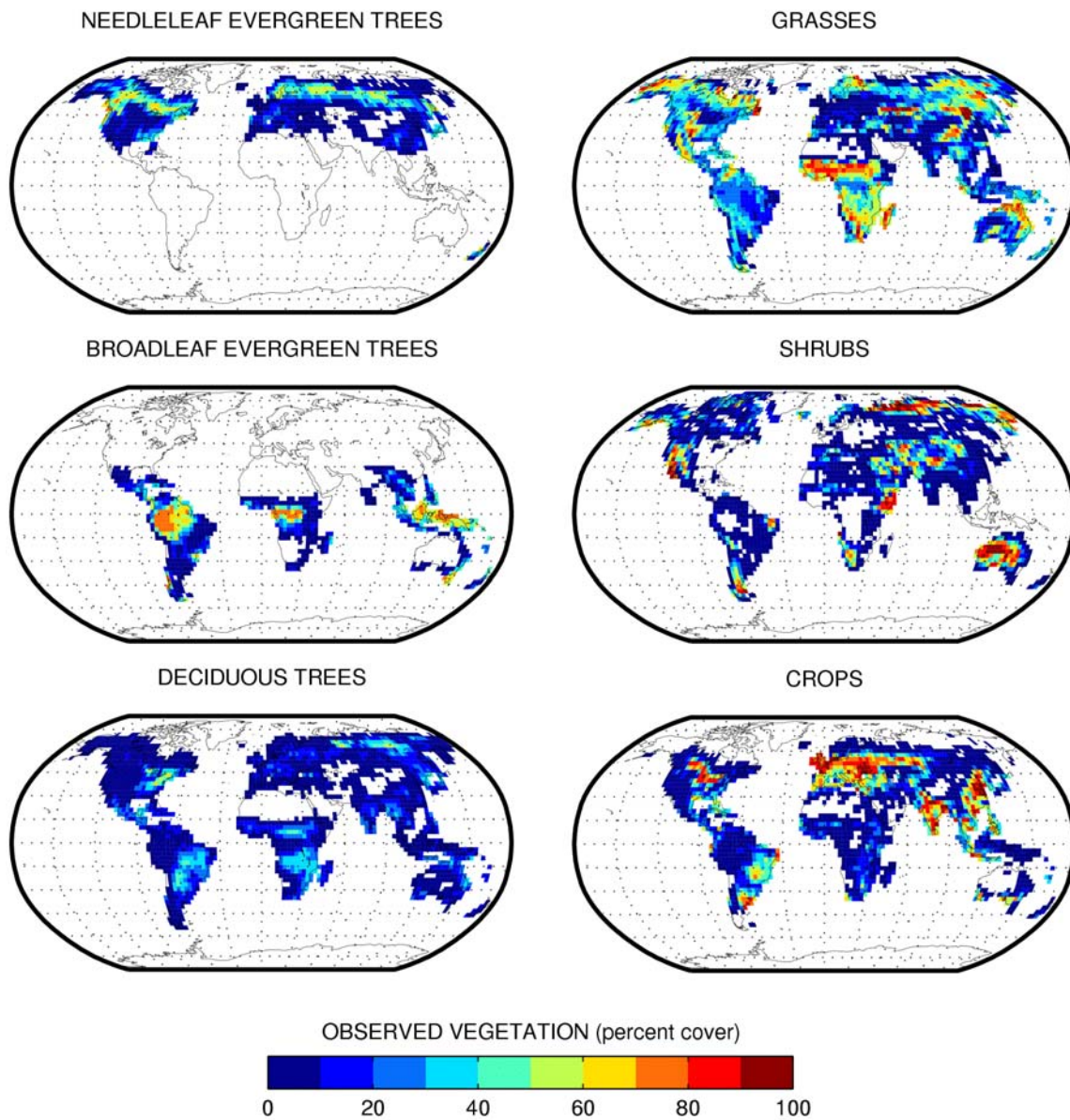


Figure 2. Observed global vegetation cover as a percentage of the soil-covered portion of the grid cell (Bonan et al. 2002b).

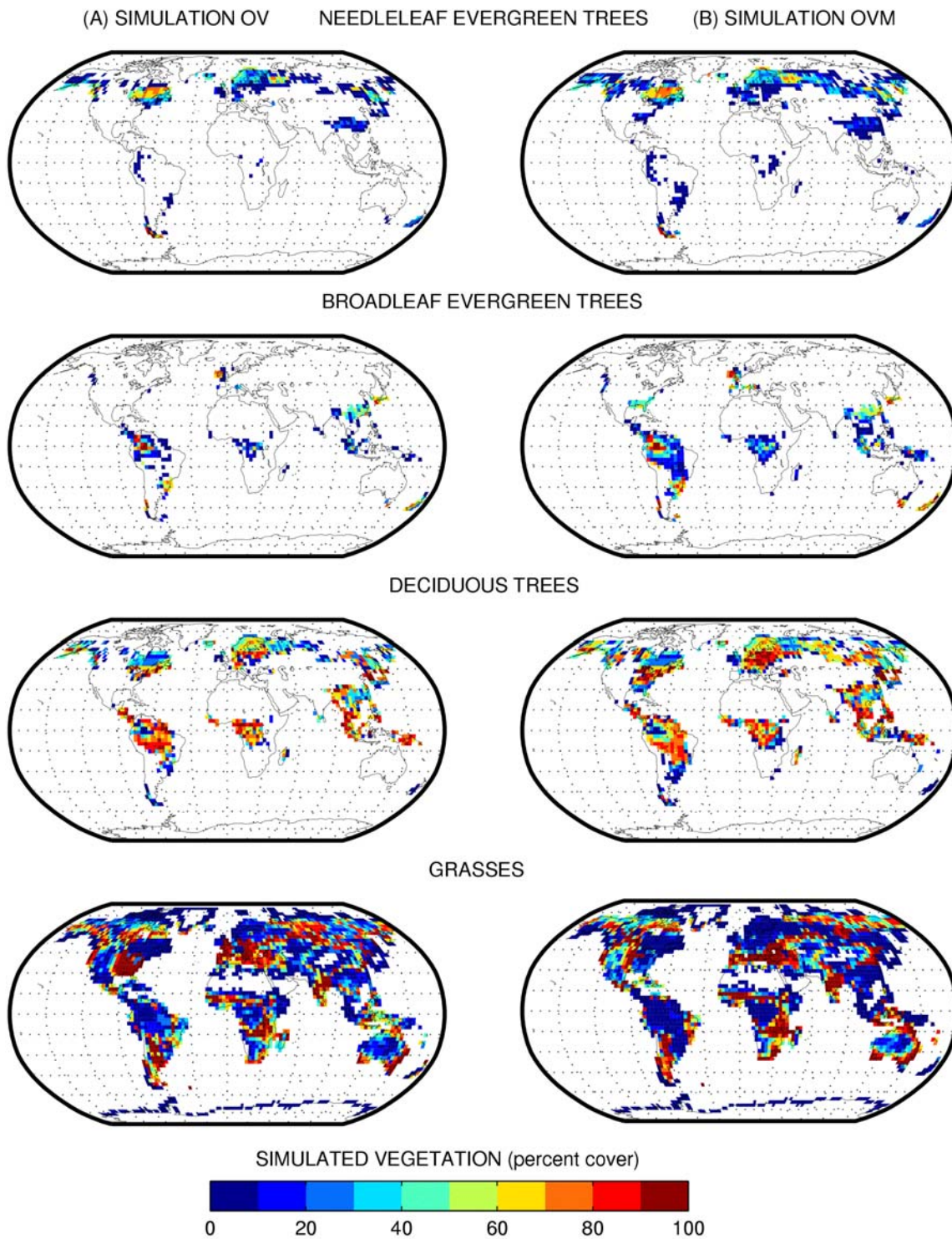


Figure 3. As in Figure 2 but for vegetation in simulations (A) OV and (B) OVM. Data are averages from the last 20 years of each simulation.

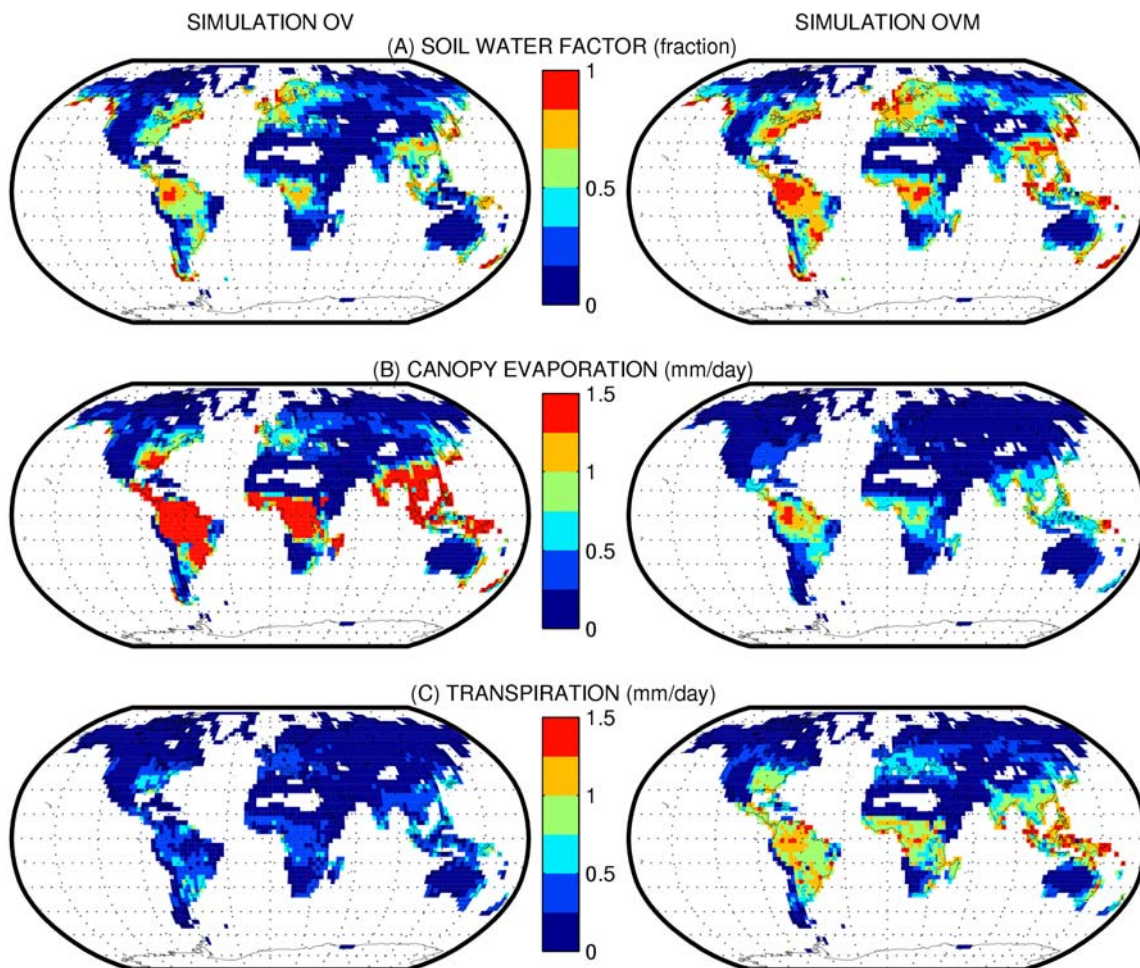


Figure 4. Annual average (A) soil water factor, β , (B) evaporation of canopy-intercepted water (mm d^{-1}), and (C) transpiration (mm d^{-1}) from simulations OV and OVM. Data are averages from the last 20 years of each simulation.

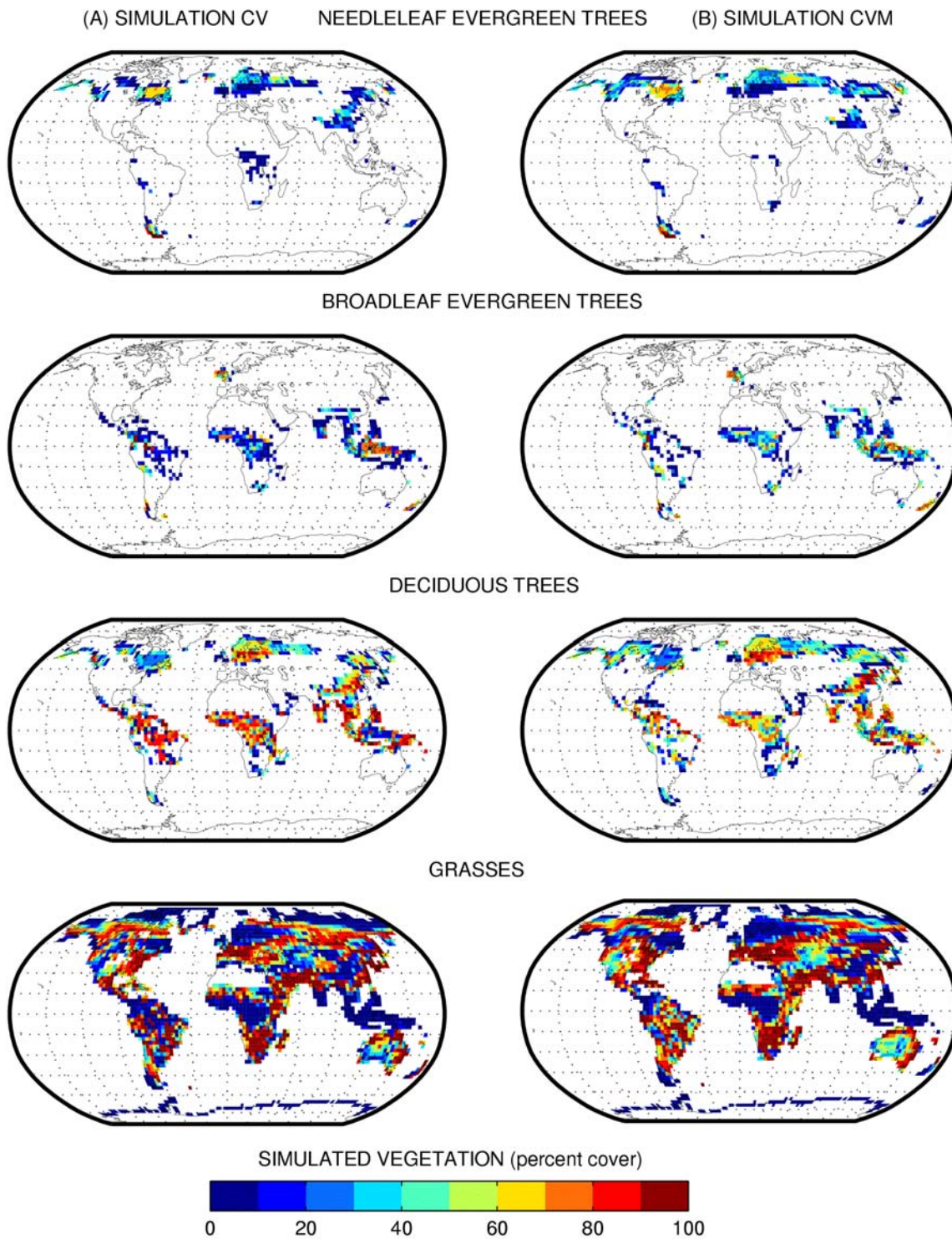


Figure 5. As in Figure 3 but for simulations (A) CV and (B) CVM.

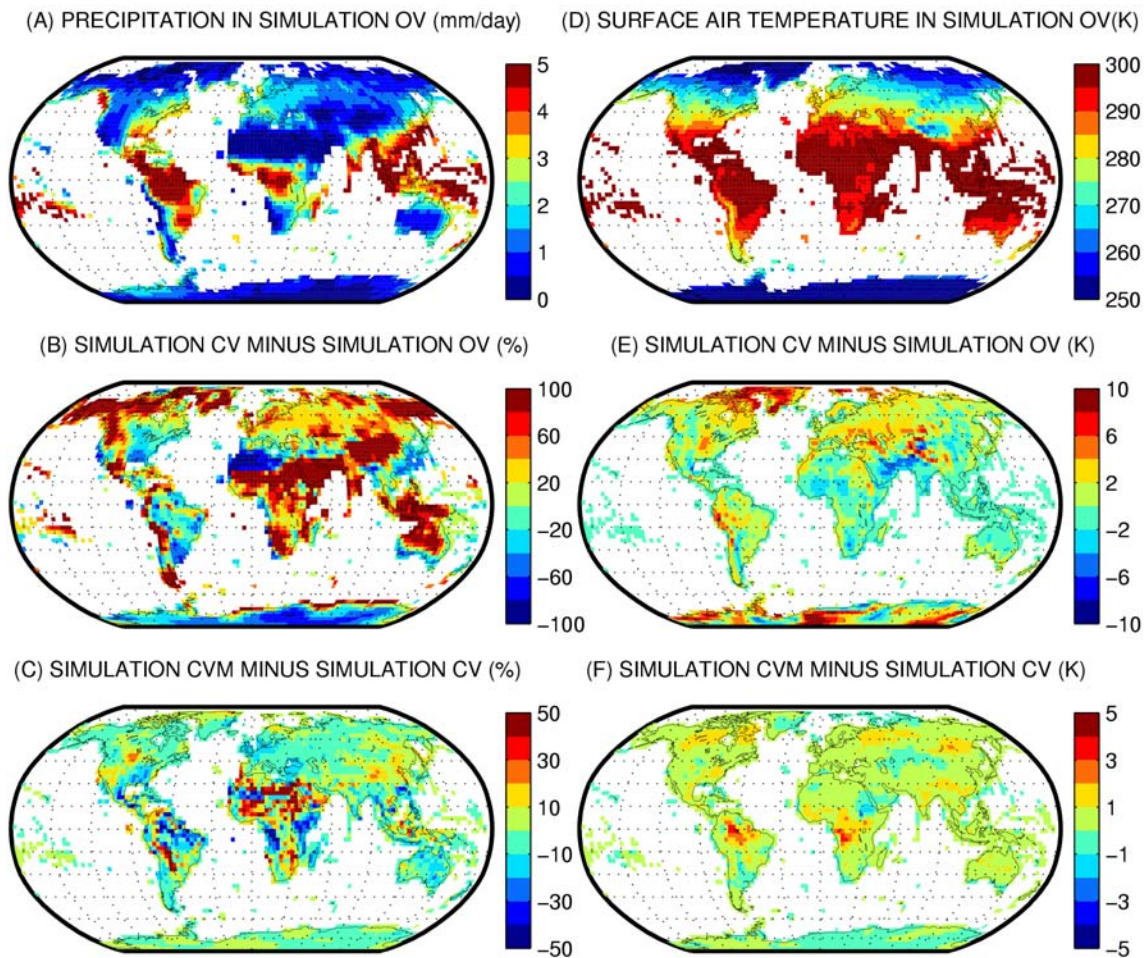


Figure 6. Annual average (A) observed precipitation from the data that drives simulations OV and OVM (Bonan et al. 2002b); (B) precipitation simulated in CV minus observed as a percent of the observed; (C) precipitation simulated in CVM minus that simulated in CV as a percent of that simulated in CV; (D) surface air temperature simulated in OV; (E) surface air temperature simulated in CV minus that simulated in OV; (F) surface air temperature simulated in CVM minus that simulated in CV. Data are averages from the last 20 years of each simulation.

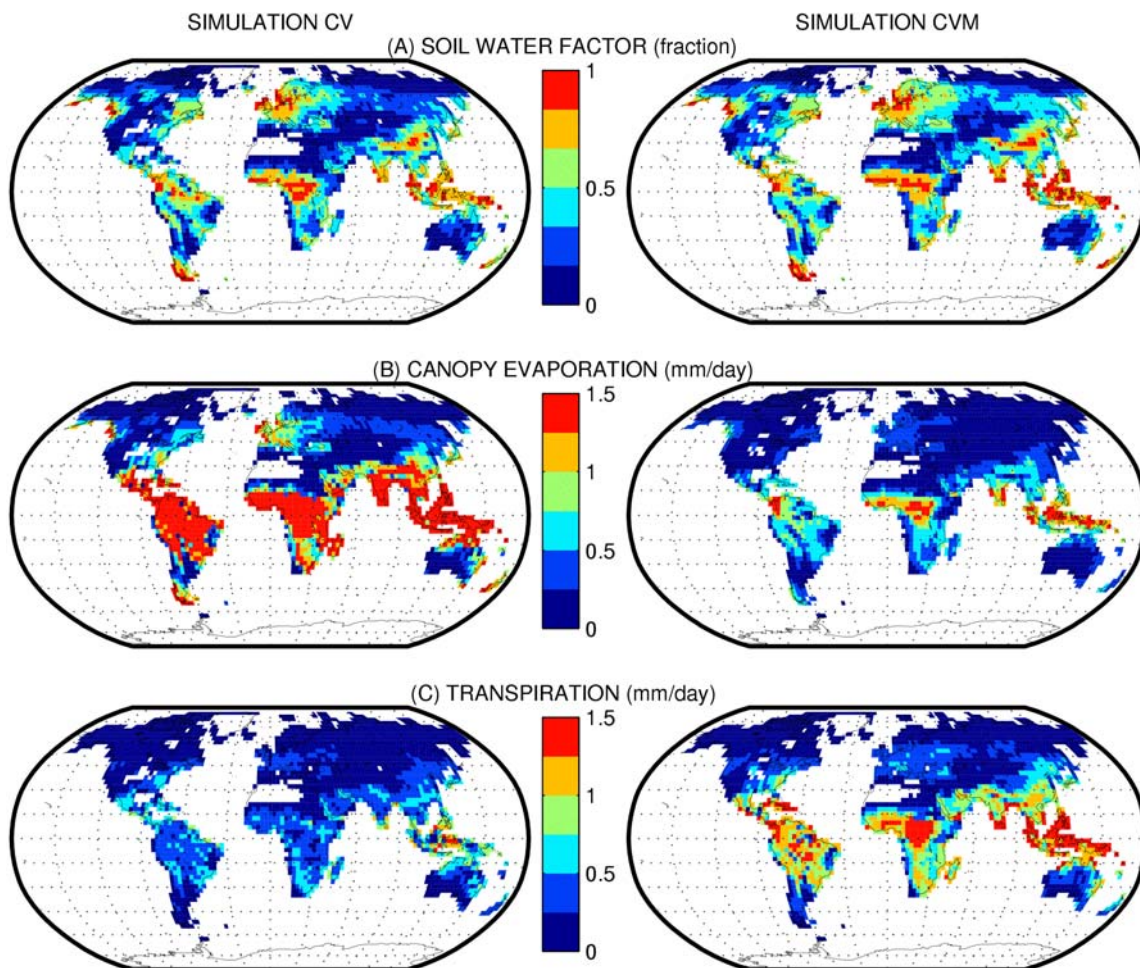


Figure 7. As in Figure 4 but for simulations CV and CVM.

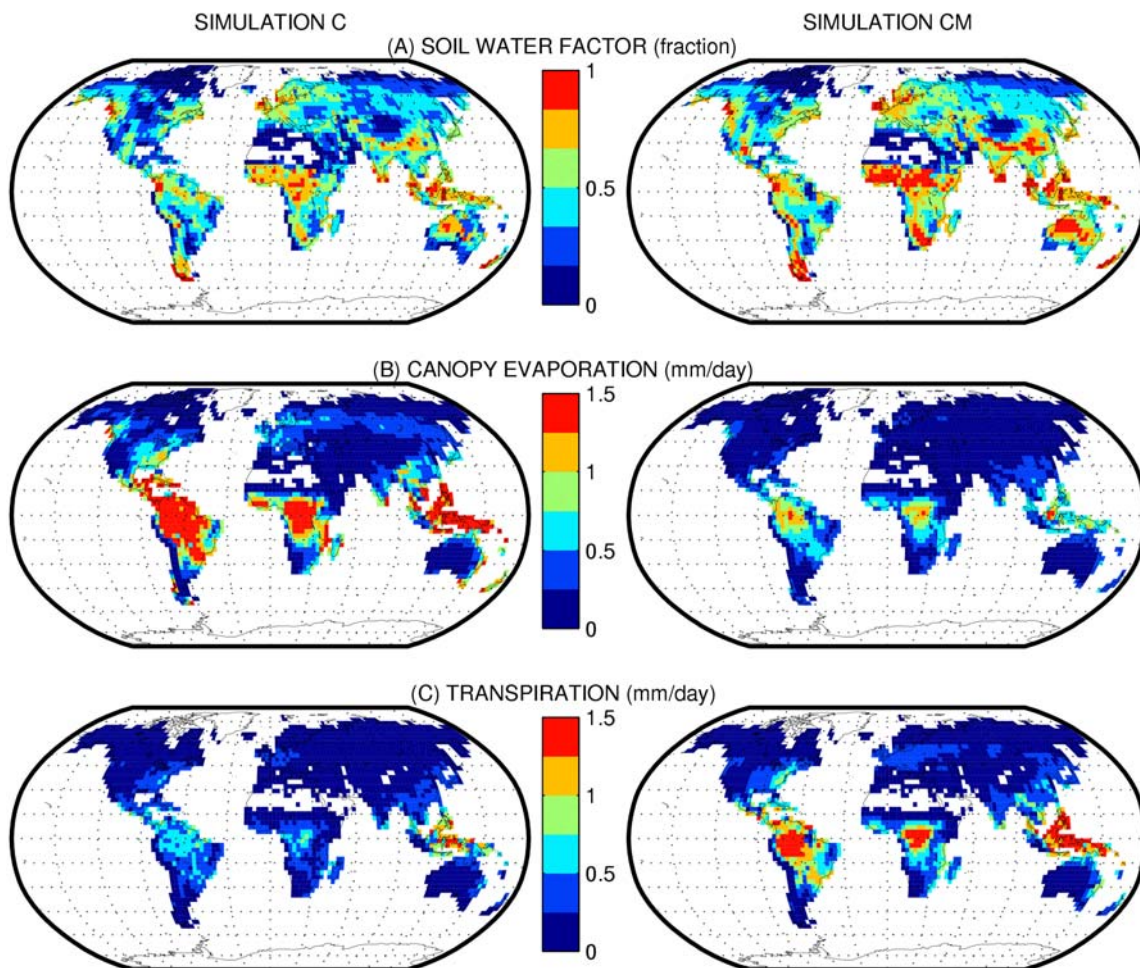


Figure 8. As in Figure 4 but for simulations C and CM.